

Absorption of CO₂ in lyotropic liquid crystals

Sandra Rodríguez-Fabià, Marita Øyen, Nicolai Winter-Hjelm, Jens Norrman, Reidar Lund, Geir Humborstad Sørland, Hanna K. Knuutila, Johan Sjöblom & Kristofer Gunnar Paso

To cite this article: Sandra Rodríguez-Fabià, Marita Øyen, Nicolai Winter-Hjelm, Jens Norrman, Reidar Lund, Geir Humborstad Sørland, Hanna K. Knuutila, Johan Sjöblom & Kristofer Gunnar Paso (2020) Absorption of CO₂ in lyotropic liquid crystals, *Molecular Crystals and Liquid Crystals*, 703:1, 87-106, DOI: [10.1080/15421406.2020.1780830](https://doi.org/10.1080/15421406.2020.1780830)

To link to this article: <https://doi.org/10.1080/15421406.2020.1780830>



© 2020 The Author(s). Published with license by Taylor and Francis Group, LLC



Published online: 09 Aug 2020.



Submit your article to this journal [↗](#)



Article views: 113






View related articles [↗](#)



View Crossmark data [↗](#)



Absorption of CO₂ in lyotropic liquid crystals

Sandra Rodríguez-Fabià^a , Marita Øyen^a, Nicolai Winter-Hjelm^a, Jens Norrman^a, Reidar Lund^b, Geir Humborstad Sørland^c, Hanna K. Knuutila^a , Johan Sjöblom^a, and Kristofer Gunnar Paso^a 

^aDepartment of Chemical Engineering, Norwegian University of Science and Technology (NTNU), Trondheim, Norway; ^bDepartment of Chemistry, University of Oslo, Oslo, Norway; ^cAnvendt Teknologi AS, Munkvollveien 56, 7022, Trondheim, Norway

ABSTRACT

Vapor-liquid equilibria data of three poly(ethylene oxide)-poly(propylene oxide)-poly(ethylene oxide)/water liquid crystals (LCs) with CO₂ has been obtained up to 6 bar. The investigated LCs consist of 60% (EO)₃(PO)₅₀(EO)₃ (Pluronic L81), 70% (EO)₈(PO)₄₇(EO)₈ (Pluronic L92), and 70% L92-NH₂. The maximum CO₂ loading of the LCs was 5–13 g CO₂/kg sample. Pure L81 and L92 displayed higher absorption of CO₂ than the LCs. Rheology measurements revealed that the increasing viscosity of the samples decreases the CO₂ loading. Water diffusion in the LCs was qualitatively investigated by nuclear magnetic resonance, confirming that free water and tightly bound water are present in the LCs.

KEYWORDS

CO₂ absorption; lyotropic liquid crystals; PEO-PPO-PEO; rheology

Introduction

CO₂ sorption in liquid crystals (LCs) has recently been investigated to assess the potential use of this technology for carbon capture and storage (CCS) purposes [1–5]. The CCS process consists of three main stages which involve capture of CO₂ produced in power plants, transportation of captured CO₂, and underground long-term storage of CO₂ in depleted oil and gas reservoirs and deep saline formations [6]. This process is considered as one of the potential solutions to reduce CO₂ emissions and to help preventing global warming [7–11].

Gas sorption in thermotropic LCs and polymeric liquid crystals (PLCs) was investigated in the 1990s, particularly CO₂ sorption experiments [12–15]. Chen et al. studied the sorption and diffusion of several gases (CO₂, N₂, Ar, and He) in LCs, and the highest gas solubility was obtained with CO₂ [14]. In the past years, there has been a growing interest in the use of LCs for CO₂ capture. For instance, the rapid phase switch of thermotropic LCs from liquid-crystalline state to isotropic state has been the basis for an alternative process for CO₂ capture designed by Gross and Jansens [1]. Moreover, de Groen et al. studied the solubility of CO₂ in thermotropic LCs, as well as the phase behavior of the LCs with CO₂, to evaluate whether the investigated systems could be

CONTACT Sandra Rodríguez-Fabià  sandra.fabia@rise-pfi.no  Department of Chemical Engineering, Norwegian University of Science and Technology (NTNU), Trondheim, Norway.

© 2020 The Author(s). Published with license by Taylor and Francis Group, LLC

This is an Open Access article distributed under the terms of the Creative Commons Attribution-NonCommercial-NoDerivatives License (<http://creativecommons.org/licenses/by-nc-nd/4.0/>), which permits non-commercial re-use, distribution, and reproduction in any medium, provided the original work is properly cited, and is not altered, transformed, or built upon in any way.

used as solvents for CCS [2–5], and for natural gas sweetening [16]. However, they concluded that further research is required in order to find LCs with higher absorption capacity [2, 4, 16]. The most interesting features of the LC technology as a potential process for CO₂ capture are the fast switch between phases, which is triggered over small temperature differences, and the abrupt change in CO₂ solubility between the isotropic and the liquid-crystalline phases [1, 5, 13, 14].

Amphiphilic block copolymers consisting of a poly(propylene oxide) (PPO) middle block and two poly(ethylene oxide) (PEO) side blocks are commercially available under the trade names Pluronic, or Poloxamer. The molecular weight and the ratio of the size of the PEO/PPO blocks of these polymers can easily be tuned, which changes the amphoteric behavior of the polymers. Due to this versatility, PEO-PPO-PEO copolymers can be used in a wide range of applications such as detergency, dispersion stabilization, lubrication, emulsification, and biomedical applications [17–22].

At high concentrations, PEO-PPO-PEO copolymers in aqueous solutions self-assemble and form lyotropic liquid-crystalline phases. The microstructure of these LCs has been extensively studied using small angle X-ray scattering [23–25]. The concentration at which the different microstructures are formed is affected by the molecular weight of the polymer, as well as the PEO/PPO ratio [24, 26, 27]. The phase behavior of three different PEO-PPO-PEO copolymers with the same PEO/PPO ratio, but different molecular weights (Pluronic L62, L92, and L122) was investigated by Svensson et al. [24]. They reported the presence of liquid-crystalline phases, including the formation of reverse hexagonal phases, which was reported for the first time in PEO-PPO-PEO/water systems.

Rheological properties of lyotropic LCs have also been documented. Robles-Vázquez et al. [28] reported the rheological properties of lamellar phases of aerosol OT (AOT) as a function concentration. They found that lamellar phases exhibit shear-thinning and power law behavior. They also measured the dynamic moduli as a function of strain amplitude, and observed that the linear viscoelastic region was limited to small strain amplitudes. From frequency sweep experiments, they concluded that the lamellar phase has an elastic nature. More recently, Mezzenga et al. [29] investigated the properties of several liquid-crystalline phases (lamellar, hexagonal, and bicontinuous cubic phases). They identified the phase transitions by the change of the dynamic moduli and studied the viscoelastic properties of the liquid-crystalline phases. They observed that when lamellar phases are under shear, the plastic behavior of the lamellar phases is due to the sliding of the lamellae while hexagonal phases have viscoelastic properties [29].

There are as well several studies on the rheological properties of PEO-PPO-PEO block copolymers, correlating them with the microstructure of the polymers [30, 31]. Prud'homme et al. [30] studied the supramolecular structure of aqueous solutions of Pluronic F127. At concentrations below 12.5 wt% the samples behave like Newtonian fluids, whereas above 17 wt% they behaved like gels. They performed small angle neutron scattering (SANS) experiments and showed that no large aggregates are formed in the samples with Newtonian behavior, because the micelles are well separated in the solution. Similarly, they also showed that samples with non-Newtonian behavior consisted of large aggregates formed by cubic packing of micelles, due to the overlap of micelle shells [30].

Hyun et al. [31] investigated the rheological properties of Pluronic F127 solutions in the linear and nonlinear viscoelastic regime. They performed large amplitude oscillatory

shear (LAOS) test, which are non-linear experiments consisting of a strain sweep test prior to a frequency sweep. From the strain sweep experiments, they concluded that complex fluids could be classified in four different categories according to their behavior outside the linear regime [32]. In type I (strain-thinning), G' and G'' decrease with increasing strain. Type II (strain-hardening) has the opposite behavior than type I: G' and G'' increase with increasing strain. Type III (weak strain overshoot): G' decreases, whereas G'' first slightly increases and then decreases. Type IV (strong strain overshoot) both G' and G'' first increase and then decrease [32]. In the case of Pluronic F127, the samples displayed different LAOS behavior depending on the temperature and the microstructure changes caused by the sol-gel transition [31].

Similarly to PEO-PPO-PEO copolymers, polyethylene oxide (PEO) has also been employed for a wide range of applications, including CO₂ capture. One of the alternatives for CO₂ absorption is the Selexol process, which uses a solvent based in PEO derivatives (polyethylene oxide dimethyl ethers) [7]. Genosorb 1753 is a similar solvent, also consisting of polyethylene oxide dimethyl ethers. Aravind et al. studied the solubility of CO₂ in a series of physical solvents, and concluded that among the solvents tested, Genosorb had the highest CO₂ solubility [33]. Moreover, Li et al. studied the solubility of CO₂ in PEOs of different molecular weights [34]. They found that the CO₂ solubility in PEO decreases with increasing temperature and decreasing pressure, and that it increases with increasing molecular weight of PEO [34–36].

Amine solvents are the most commonly used for post-combustion capture of CO₂ by chemical absorption. Therefore, new amine-functionalized technologies for CO₂ capture, such as zeolites, metal-organic frameworks, and membranes have been developed to enhance the absorption capacity and selectivity of the materials [9, 37–40]. Modification of PEO end groups to amines can be achieved by several synthetic methods typically requiring several reaction steps. Harris et al. described a two-step method to modify hydroxyl end groups in PEO polymers to amines via aldehyde formation [41]. Similarly, Gyulai et al. employed this synthesis to modify the end groups of PEO-PPO-PEO copolymers to amines [42].

In this work, we investigate the CO₂ absorption of lamellar liquid-crystalline phases of Pluronic L81, L92, and hexagonal phases of amine end-group modified L92 (L92-NH₂). The vapor–liquid equilibrium (VLE) data of the LCs has been compared with the behavior of the pure polymers (L81 and L92). To our knowledge, the absorption capacity of pure Pluronic, Pluronic/water LCs, and modified Pluronic have not been investigated before. Moreover, the rheological properties of the samples were also studied. Both the absorption and rheology experiments provide information on the effect of the end group modification, which *a priori* was expected to improve the absorption capacity of the samples, although the experimental results proved that it was not the case. In addition, the water diffusion in the LCs was investigated using low-field NMR, which gives an indication of how tightly water is bound to the polymers, and the possibility of CO₂ to penetrate the core of the LCs.

Materials and methods

Materials

Pluronic L92 (poly(ethylene oxide)-poly(propylene oxide)-poly(ethylene oxide) (PE 9200, $M_n \approx 3650$ g/mol, 20 wt% PEO) was provided by BASF Corporation

(Ludwigshafen, Germany). Pluronic L81 (PE 8100, $M_n \approx 2800$ g/mol, 10 wt% PEO) was purchased from Sigma Aldrich (Saint Louis, MO, USA). The composition of Pluronic L92 and Pluronic L81 can be represented as $(EO)_8(PO)_{47}(EO)_8$ and $(EO)_3(PO)_{50}(EO)_3$, respectively [24, 43]. Acetic anhydride ($\geq 98.0\%$), Schiff's reagent for aldehydes, ammonium chloride ($\geq 99.5\%$), sodium cyanoborohydride (95%), fluorescamine ($\geq 98.0\%$), sodium tetraborate decahydrate ($\geq 99.5\%$), hexylamine (99%), diethyl ether, and methanol ($\geq 99.8\%$) were purchased from Sigma Aldrich. Carbon dioxide (gas, 99.9%) was purchased from AGA AB (Stockholm, Sweden). Potassium hydroxide was purchased from Merck KGaA (Darmstadt, Germany). DMSO ($\geq 99.9\%$) was purchased from Acros Organics (Geel, Belgium), and acetone ($\geq 99.5\%$) was purchased from Honeywell Chemicals (Charlotte, NC, USA). All chemicals were used as received. Milli-Q water was used as solvent (18.2 M Ω cm at 25 °C). 3 Å molecular sieves were purchased from Fluka Chemie GmbH (Buchs, Switzerland) and pre-dried at 300 °C for 24 h [44]. Compositions of liquid-crystalline samples are expressed in weight %.

Synthesis and characterization of pluronic L92-NH₂

Pluronic L92 was modified following the methods described by Harris et al. [41] and Gyulai et al [42]. DMSO was dried by allowing it to stand on 3 Å molecular sieves during 24 h under nitrogen atmosphere [44]. 30 g L92 (8.2 mmol) were dissolved in 90-mL dry DMSO. 2.25 g (22.0 mmol) acetic anhydride were added, and the reaction mixture was stirred for 30 h at room temperature. The reaction was stopped by pouring the reaction mixture into cold diethyl ether. The presence of aldehydes was checked using Schiff's reagent. A small sample was taken from the reaction mixture and a few drops of Schiff's reagent were added. The reagent turned pink, confirming the presence of aldehyde groups. The sample was dialyzed against distilled water for 7 days using dialysis tubes with molecular weight cut off 1 kDa (Spectra/Por® 7, Spectrum). After dialysis, the sample was isolated by freeze drying.

26 g L92-CHO (7.1 mmol), 7.65 g (143 mmol) ammonium chloride and 0.95 g (16.9 mmol) KOH were dissolved in 215 mL methanol. 9.42 g (149.9 mmol) sodium cyanoborohydride were dissolved in 220 mL methanol and added dropwise to the reaction mixture over 30 min. 4.76 g (84.8 mmol) KOH were added to the reaction mixture, and the solution was stirred for 24 h at room temperature. The reaction was stopped by pouring the solution into diethyl ether, and the polymer was purified by dialysis against distilled water for 7 days in 1 kDa molecular weight cut off dialysis tubes (Spectra/Por® 7, Spectrum), and was then freeze dried. L92-NH₂ was used to prepare samples with a composition of 70% L92-NH₂ and 30% water.

Fluorescamine assay

Conversion of end groups to amines was quantified by the fluorescamine assay [42]. L92-NH₂ samples with concentration 0.2 g/L were prepared in 0.1 M sodium tetraborate buffer solution with pH 9. pH was measured with a Seven Easy S20 pH-meter (Mettler Toledo, Columbus, OH, USA). 0.3 g/L fluorescamine solution in acetone was prepared. In order to measure the fluorescence spectra of L92-NH₂, three parallels with 250 μ L fluorescamine solution were dissolved in L92-NH₂ buffer solution up to a volume of

5 mL. Similarly, a 0.2 g/L hexylamine sample was prepared in 0.1 M sodium tetraborate buffer solution. 5 mL samples of 250 μ L fluorecamine solution dissolved in hexylamine buffer solution were used as reference to calculate the degree of conversion of the end groups in the L92-NH₂ samples. Fluorescence spectra were obtained with a Fluorolog-3 spectrofluorometer (HORIBA Jobin Yvon, Bensheim, Germany), with excitation and emission wavelengths $\lambda_{\text{ex}}=390$ nm and $\lambda_{\text{em}}=405$ nm. Monochromator slit widths were set at 5 and 3 nm, respectively. The measurements were performed in quartz cuvettes.

Small angle X-ray scattering (SAXS)

The structure of 70% L92-NH₂ was determined by SAXS measurements performed on a Bruker Nanostar SAXS. The system is equipped with a Vântec-2000 detector (Bruker AXS GmbH, Karlsruhe, Germany). K α radiation ($\lambda = 1.54$ Å) was provided by an I μ S Cu microsource (Incoatec, Geesthacht, Germany) operating at 50 kV and 60 mA. The measurements were performed in a sandwich cell with Kapton windows at controlled temperature. The raw scattering data were calibrated to absolute intensity using water as standard. The radial average of the scattering data provided the 1-D scattering profile as a function of the scattering vector. The scattering of the empty cell was measured and subtracted from the corresponding sample measurements. Experiments were conducted from 15 to 50 °C at 5 °C intervals. An additional measurement was performed at 25 °C after cooling down from 50 °C.

The microstructure of 70% L92-NH₂ was determined from the relative positions of the SAXS diffraction peaks [24, 45]. The peak positions of lamellar phases follow the relationship 1:2:3:4..., whereas the peak positions of hexagonal structures follow the ratios 1: $\sqrt{3}$:2: $\sqrt{7}$:3... The position of the most intense diffraction peak (Q) was used to calculate lattice parameters of the lamellar (1) and hexagonal (2) aggregates using the following equations:

$$Q = \frac{2\pi}{d} \quad (1)$$

$$Q = \frac{4\pi}{a\sqrt{3}} \quad (2)$$

where, d is the lamellar periodicity, a is the distance between centers of adjacent cylinders.

Vapor liquid equilibrium (VLE) experiments

CO₂ loading of samples consisting of 60% L81, 70% L92, 70% L92-NH₂, pure L92, and pure L81 was investigated using a CPA202 reaction calorimeter (ChemiSens AB, Lund, Sweden). Samples were prepared by weighing corresponding amounts of polymer and Milli-Q water into a beaker and stirring the mixture manually. Most of the sample was immediately used for VLE experiments, and a small portion was kept in a closed vial to perform rheology tests. The sample was transferred into the calorimeter and used to perform the VLE experiments. A more detailed description of the setup is found in a publication by Evjen et al. [46]. The calorimeter is a glass reactor equipped with a

stainless steel lid, and it has a total volume of $258.8 \pm 0.2 \text{ cm}^3$. The reactor includes a Pt-100 temperature sensor (accuracy $0.1 \text{ }^\circ\text{C}$), a SENSIT pressure gauge (1–10 bar, accuracy 0.15% FS), and a propeller stirrer. The operation parameters, such as the reactor temperature and pressure, the CO_2 temperature and pressure, and the heat flow, were recorded using ChemiCall software from Chemisens. In order to control the temperature, the experiments are conducted in a CPA202BU Thermostat filled with diethylene glycol as heating medium. The CO_2 flow injected to the reactor was controlled with a mass flow controller (0.5 nL/min , Bronkhorst[®] Hightech).

The experiments were performed at isothermal conditions ($30 \text{ }^\circ\text{C}$). Approximately 120 g of sample were used in each experiment, except in the case of 70% L92- NH_2 , where ca. 80 g of sample were used. The reactor was in vacuum prior to CO_2 addition. Several CO_2 injections that lasted 10 s were performed, until the pressure in the reactor reached 6 bar. After each injection, the system was allowed to equilibrate until predefined stability conditions were reached, and the system stayed in that state for 10 min. The stability conditions were set to a pressure difference of $\pm 5 \text{ mbar}$, and a temperature difference of $\pm 0.5 \text{ }^\circ\text{C}$. After the reactor pressure reached 6 bar and stability conditions were reached, the samples were allowed to equilibrate for 8 h before the experiment was finished.

Cross-polarized visual inspection

Birefringence of the samples was tested by visual observation of all samples between cross-polarizers. Lamellar and hexagonal phases are anisotropic, and when observed under polarized light they are birefringent. On the other hand, cubic phases and liquids are isotropic and therefore are not birefringent.

Rheology

Rheological measurements were performed using a Physica MCR 301 rheometer (Anton Paar, Graz, Austria). Sandblasted cone-and-plate geometry was used for samples 70% L92, 70% L92- NH_2 and the corresponding samples after absorption of CO_2 . The cone angle was 2.009° and its radius was 39.975 mm. Due to lower viscosity of the samples, double gap geometry was used for 60% L81 (+ CO_2), 100% L81, and 100% L92. The inner diameter of the cylinder was 23.828 mm and the external diameter 27.987 mm. The viscosity was measured as a function of the shear rate between 0.01 and 1000 s^{-1} . Oscillatory measurements were performed to determine viscoelastic behavior. The elastic (G') and loss (G'') moduli were measured as a function of strain amplitude at a frequency of 1 Hz. The strain amplitude range was 0.001–10%. Frequency sweep of the elastic modulus (G') and the loss modulus (G'') was performed at a strain amplitude of 0.1% with a frequency range of 0.1–100 Hz. All measurements were performed at $25 \text{ }^\circ\text{C}$.

NMR

The pulsed field gradient (PFG) NMR technique was applied to measure diffusion within a sample of 20 mm height and 18 mm in diameter. The NMR instrumentation consisted of a permanent magnet, 21 MHz in proton frequency, supplied by Anvendt

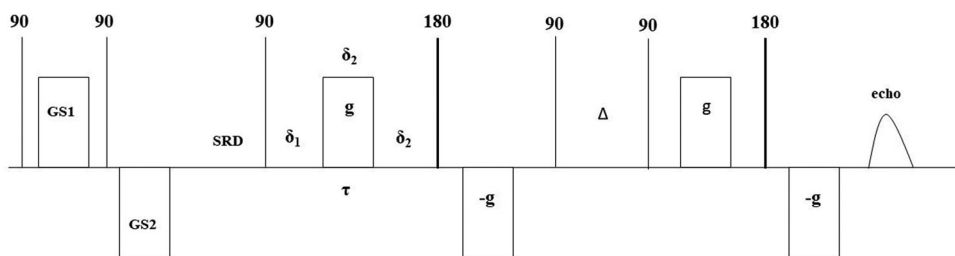


Figure 1. The 13 interval PFGSTE sequence with a spoiler recovery sequence prior to the diffusion sequence.

Teknologi AS (Trondheim, Norway, www.antek.no) with magnetic field gradient accessories capable of delivering up to 320 G/cm in applied magnetic field gradient strength. The PFG-NMR sequence used to measure diffusion was the 13 interval sequence [47] as shown in Fig. 1.

Here $\text{SRD} = 4 \text{ s}$, $\delta_1 = 0.2 \text{ ms}$, $\delta = 1.5 \text{ ms}$, $\delta_2 = 0.8 \text{ ms}$, and $\Delta = 50 \text{ ms}$. The strength, g , of the PFG varied from 2.4 G/cm and up to 220 G/cm in 24 increments. The spoiler gradients GS1 and GS2 were set to 2.1 G/cm and -3.4 G/cm in order to spoil any magnetization prior to the recovery delay SRD [48, 49]. The acquired diffusion data were processed using an inverse Laplace transform.

Results and discussion

The concept of CO_2 capture in LCs is illustrated in Fig. 2. The choice of Pluronic (molecular weight, PEO/PPO ratio) has a strong influence on the final properties of the LCs. In the presence of water, these amphiphilic polymers self-assemble into aggregates, which, under the adequate conditions, namely concentration and temperature, form lyotropic LCs. Bubbling of CO_2 through the LCs allows the absorption of the CO_2 molecules by polar interactions with water and the ether groups of the polymers.

In our previous work, we reported the CO_2 absorption of a liquid-crystalline system consisting of Pluronic L92/ethanolamine/water [50]. LCs containing ethanolamine were of interest because this solvent is typically used to absorb CO_2 . In this article, we want to study the absorption capacity and phase behavior of LCs that have the amine groups attached to the polymer molecules, instead of the effect of amines added to the system as a solvent.

Synthesis and characterization of L92-NH₂

An amine end-group modified derivative of Pluronic L92 (L92-NH₂) was prepared via a two steps synthesis consisting of first oxidation of the hydroxyl end groups to aldehydes, and then reductive amination of the aldehyde groups. The reaction scheme is shown in Fig. 3.

Since a large amount of L92-NH₂ was required for the VLE experiments, the synthesis was carried out in several batches. The overall yield of the modification was 59–67%. These results are in agreement with the yields reported for other types of Pluronic, which were 60–80% [42]. The yields obtained after the first step of the modification were between 80% and 90%. The presence of aldehyde groups was confirmed by Schiff's test, although the degree of conversion could not be calculated. The yield of the second

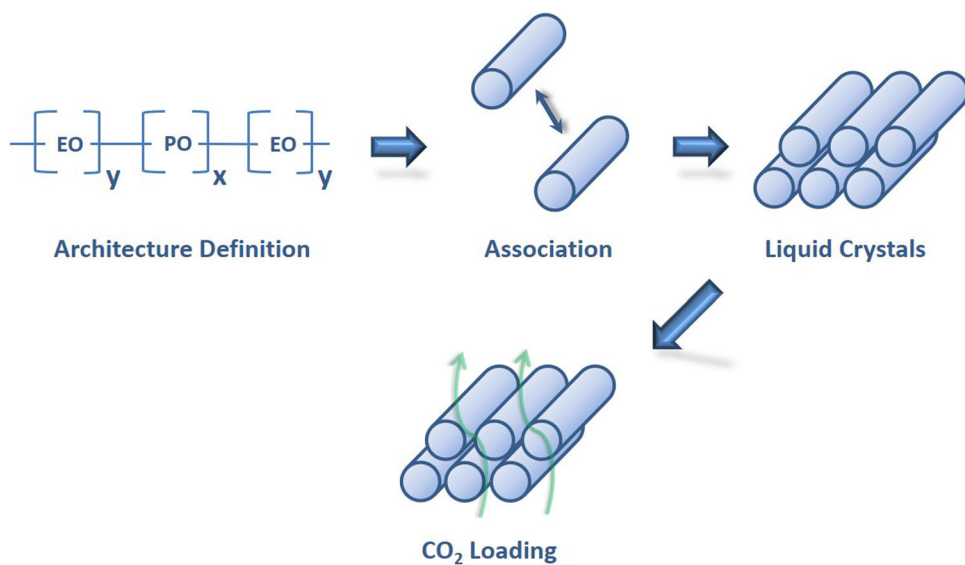


Figure 2. Schematic illustration of carbon dioxide absorption in the liquid crystal system.

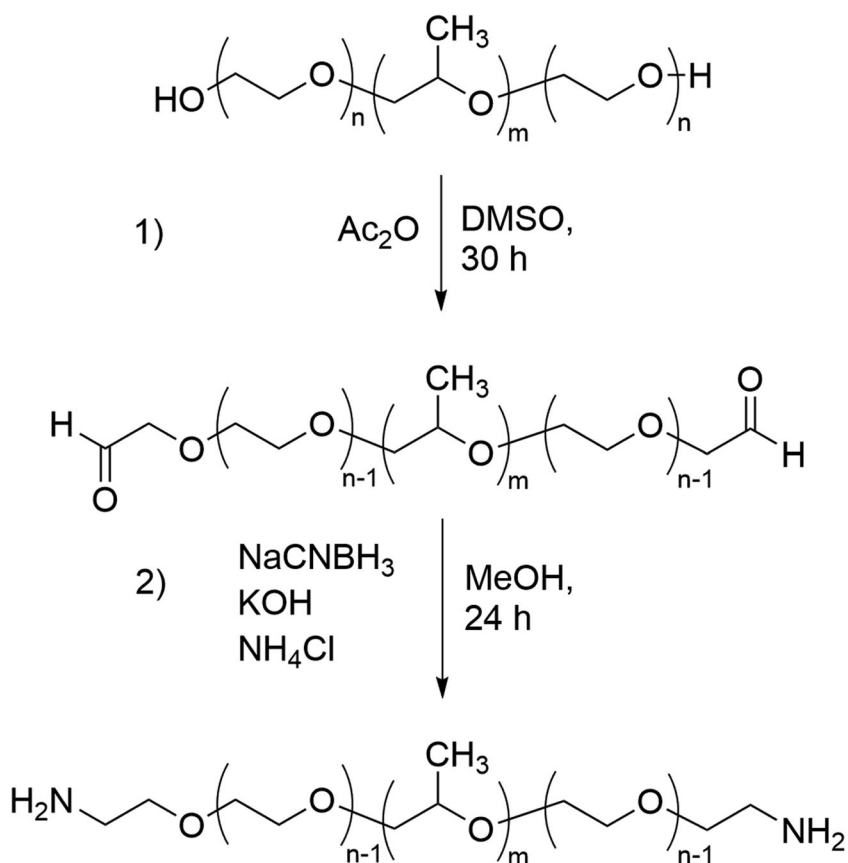


Figure 3. Reaction scheme of the amine end group modification of Pluronic.

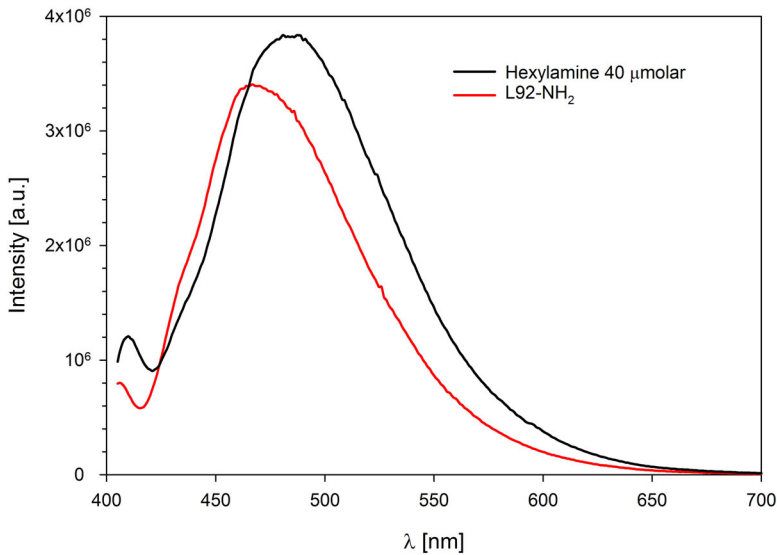


Figure 4. Fluorescence spectra of 40 μmolar hexylamine and L92-NH₂.

step of the modification was between 74% and 78%. The overall conversion of hydroxyl end groups to amines was calculated from the fluorescamine assay, as described by Gyulai et al. [42]. The average maximum intensity of the fluorescence spectra of the L92-NH₂ sample was found at 467 nm (Fig. 4).

Hexylamine solutions with concentrations 0–60 $\mu\text{mol/L}$ were used to make a calibration curve to quantify the amine end groups by plotting the intensities recorded at 467 nm. The amine concentration of all batches combined was found to be 38 $\mu\text{mol/L}$, which is equivalent to 34% conversion of the end groups. The reported end group conversions for Pluronic F68, F108 and F127 vary between 22 and 41% [42], which are in agreement with the 34% average conversion obtained in this work. The apparent yield of the fluorophore formation reaction is dependent on the structure of the amines, therefore, the calculated end group conversion should be considered as an approximate value [42, 51].

Fig. 5 shows the SAXS profile of 70% L92-NH₂. A clear transition from lamellar structure to hexagonal is observed from 20 to 25 °C. It should be noted that with the SAXS data it is not possible to distinguish between hexagonal and reverse hexagonal phases. Considering that unmodified L92 forms reverse hexagonal phases at a concentration of ca. 80% (while normal hexagonal phases are formed at concentrations between 40% and 50%), and that by increasing the temperature the solubility of the polymer decreases, it is reasonable to assume that in this case reverse hexagonal phases are formed [24, 45]. At 15 and 20 °C the sample self-assembles into lamellar aggregates. Upon further heating, the sample forms hexagonal aggregates. The microstructure remains unchanged, until 50 °C is reached, where due to the high temperature and the increased mobility of the molecules, the peaks start to broaden, indicating the loss of short-range order among the molecular aggregates. At 30 °C, 70% L92 forms lamellar aggregates, whereas the modified polymer forms hexagonal aggregates. This difference in microstructure could be caused by the addition of amine groups to the polymer, as well as the loss of the most hydrophilic polymer chains present in the sample due to the dialysis process.

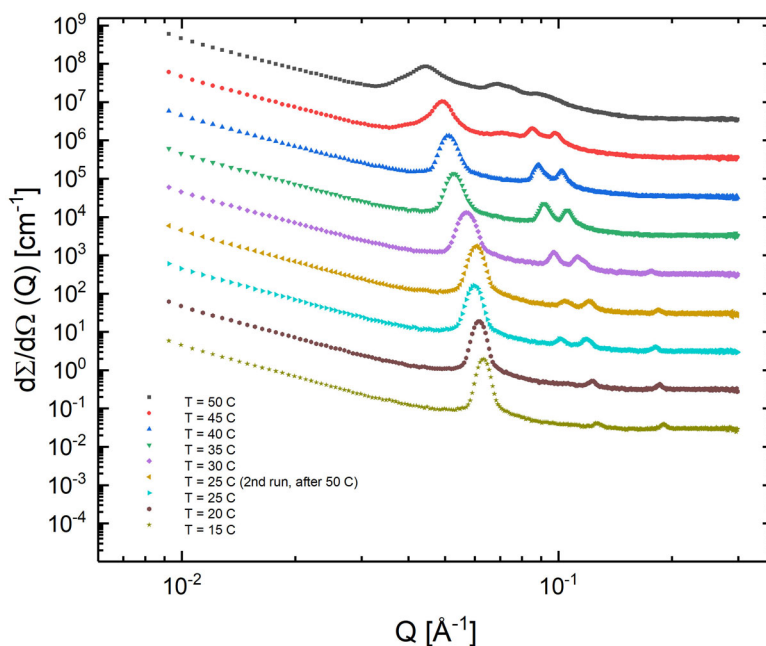


Figure 5. SAXS spectra of L92-NH₂ at various temperatures.

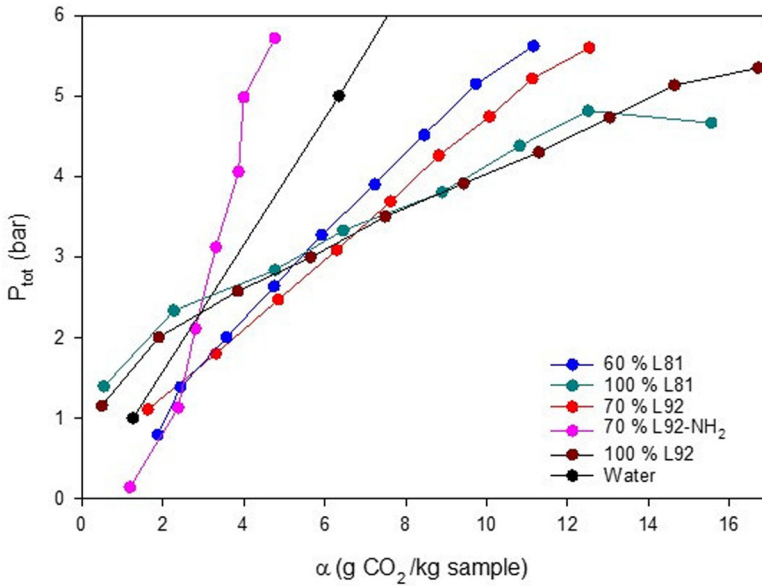
The lattice parameters of 70% L92-NH₂ at various temperatures were calculated and are shown in Table 1. As temperature increases, the lattice parameters increase, most likely due to the higher mobility of the molecules, leading to a looser packing of the aggregates. It should be noted that although the lattice parameters have been calculated at 50 °C, the microstructure of the sample at this temperature is not as well defined as for other temperatures.

VLE experiments

The results of the loading of the samples after each CO₂ injection are shown in Fig. 6, where the total pressure in the reactor (P_{tot}) is plotted as a function of the CO₂ loading (α). The total pressure is the sum of the partial pressure of CO₂ and the vapor pressure of the LC. However, the experiment temperature was low (30 °C), and the vapor pressure of the LCs is very small compared with the total pressure, justifying the assumption that $P_{\text{tot}} \cong P_{\text{CO}_2}$. Two different samples forming lamellar phases were chosen: 70% L92, and 60% L81 [24, 52]. The effect of modified amine end groups was investigated by measuring CO₂ absorption of 70% L92-NH₂. As a reference, the absorption of pure L92 and pure L81 was also investigated. After the pressure in the reactor has reached 6 bar, the CO₂ loading of L81 samples was 11.2 g CO₂/kg sample for 60% L81, and 15.5 g CO₂/kg sample for 100% L81. For L92 samples, the loading obtained was 12.5 g CO₂/kg sample for 70% L92, 16.7 g CO₂/kg sample for 100% L92, and 4.8 g for 70% L92-NH₂. The absorption of samples containing L92 is slightly higher than the absorption of samples with L81, most likely due to the longer PEO blocks in L92, which have affinity for CO₂ and increase the hydrophilicity of the sample [34, 36, 53].

Table 1. Lattice parameters of 70% L92-NH₂.

Temperature (°C)	Lattice parameters (Å)
15	d = 99.3
20	d = 102.7
25	a = 121.4
25 (2nd run, after 50 °C)	a = 120.0
30	a = 127.5
35	a = 137.5
40	a = 141.7
45	a = 147.8
50	a = 164.5

**Figure 6.** VLE data for 60% L81, 100% L81, 70% L92, 70% L92-NH₂, 100% L92, and water (data reproduced from Duan et al. [63]).

The VLE data show that all samples follow the same general trend: the partial pressure of CO₂ in the reactor increases linearly as the loading of the samples increases. This behavior is consistent with typical physical absorption, which is characteristic of poly(ethylene oxide) derivatives [33, 34]. The CO₂ absorption capacity of the tested materials is similar to that of water. 70% L92-NH₂ shows the lowest CO₂ absorption, although the polymer has been modified with amine end groups to promote CO₂ absorption through the reaction with amine groups [54]. It should be considered that the overall concentration of amine groups in the sample is very low. Moreover, the modified polymer has hexagonal microstructure at 30 °C, which is known to have higher viscosity than lamellar phases [55]. A similar behavior was observed by Aschenbrenner et al. in the case of CO₂ absorption in poly(ethylenimine). They reported that despite the high concentration of amine groups in poly(ethylenimine), CO₂ absorption was very slow and the system required a long time to reach equilibria due to the high viscosity of the polymer [53].

The CO₂ loading could also be affected by the ionic strength of the system. Modification of the polymer to amines, and addition of CO₂ to polymer/water systems

can lead to the formation of charged species, such as carbonic acid, or carbamate and ammonium ions from the reaction between the amine end-groups and CO_2 . The variation in ionic strength compared with the pure polymer systems, and potential adsorption of charged species at the polymer/water interface might also contribute to the change in viscosity by changing the organization of the polymer molecules, and therefore decrease the CO_2 adsorption. In spite of the low CO_2 loadings obtained for all the analyzed samples, the results are in agreement with data available for other LC systems, where the absorption of the LCs at 5 bar is below 20 mg $\text{CO}_2/\text{g LC}$ [12, 14].

Rheology

Viscosity

Lamellar liquid-crystalline samples were prepared from L81 and L92, and hexagonal LCs from L92-NH₂ [24, 52]. In addition, inspection of the samples through polarized light and SAXS measurements confirmed the presence of liquid-crystalline phases. The viscosities of the liquid-crystalline samples 60% L81, 70% L92 and 70% L92-NH₂ are shown in Fig. 7a, together with the viscosities of the isotropic samples 100% L81 and 100% L92. The viscosities of the three LCs after CO_2 absorption are plotted in Fig. 7b, and are virtually the same as the viscosities measured before the CO_2 -loading experiment due to the loss of physically trapped CO_2 by the applied shear. Before and after CO_2 -loading, the three liquid-crystalline samples exhibit shear-thinning behavior typical for lamellar and hexagonal phases and large aggregates [28, 30]. The viscosity decrease of the liquid-crystalline samples with increasing shear is caused by the breakage of the entanglements between aggregates, the destruction of the aggregates, and the alignment of the polymer molecules in the direction of the applied shear [32, 56–58]. On the other hand, the two isotropic samples follow Newtonian behavior because the pure polymers are in an isotropic state, and the lack of water means no aggregates can form [28, 30].

In general, samples containing L92 show slightly higher viscosity than samples containing L81, but the amine-modified sample displays the highest viscosity. The difference in viscosity between L92 samples and L81 is most likely due to the molecular weight of the polymers: lower molecular weight leads to lower viscosity of the samples. In addition to having a lower molecular weight, 60% L81 contains more water than both L92 samples. On the other hand, the high viscosity of 70% L92-NH₂ is due to the formation of hexagonal LCs, which are more viscous than the corresponding lamellar phases [55]. Moreover, during the modification of L92 to L92-NH₂, the polymer was purified by dialysis twice, which could have altered the average molecular weight of the polymer due to the loss of the smaller molecules.

The CO_2 absorption capacity of the samples appears to be related to their viscosity. The higher the viscosity of the sample, the more difficult it is for CO_2 to diffuse through the solvent [53]. The information of the SAXS data combined with the rheology measurements provides an explanation for the unexpectedly low absorption of the modified polymer. The presence of amine end groups was supposed to enhance the absorption capacity of the LCs. However, due to the formation of hexagonal aggregates at 70% concentration, the viscosity of the sample was higher than the one of the unmodified equivalent (70% L92), leading to a reduced CO_2 absorption. Even though

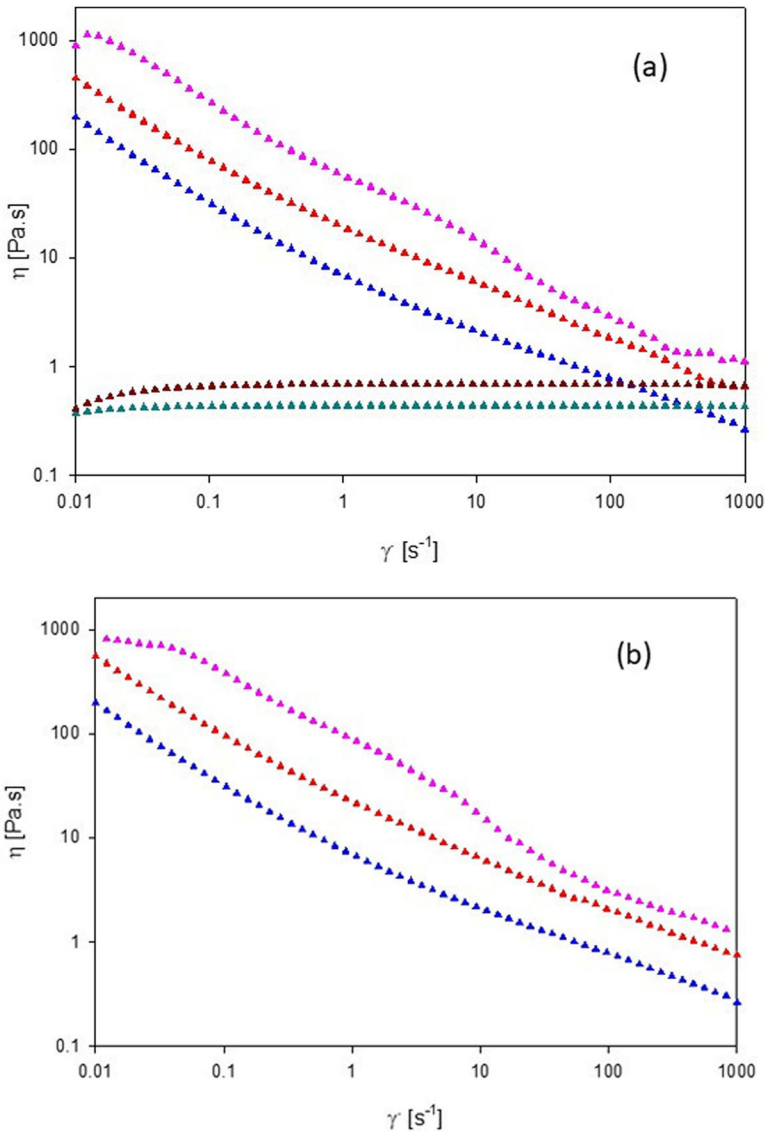


Figure 7. Viscosity (η) as a function of shear rate ($\dot{\gamma}$) of (a) 60% L81 (●), 100% L81 (●), 70% L92 (●), 70% L92-NH₂ (●), and 100% L92 (●), and (b) 60% L81 (●), 70% L92 (●), 70% L92-NH₂ (●) after CO₂-loading.

L81 samples have lower viscosity than L92 samples, the loading of 60% L81 compared to 70% L92, and 100% L81 to 100% L92, is lower, most likely due to the shorter PEO blocks in L81, which have affinity for CO₂.

Oscillatory experiments

Strain sweep. In Fig. 8 the storage and loss modulus (G' and G'') of the three liquid-crystalline samples have been plotted as a function of the strain amplitude. All samples show linear viscoelastic behavior until approximately 1% strain. The crossovers between

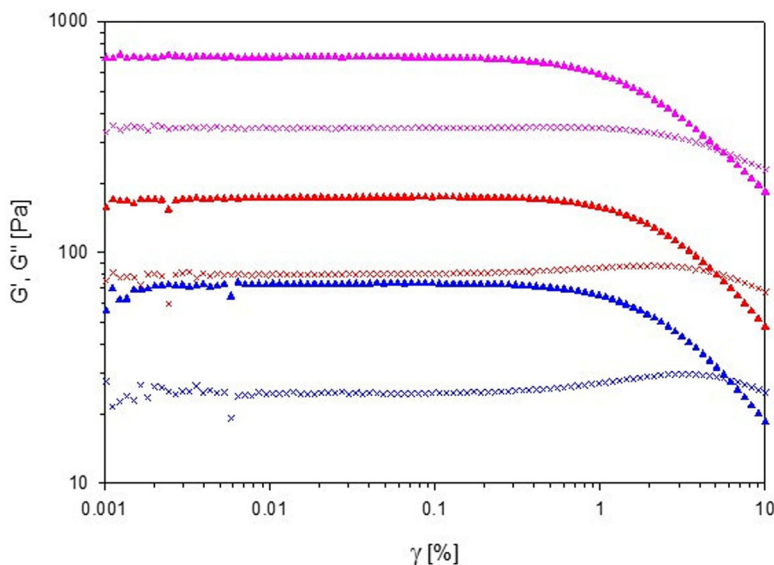


Figure 8. Storage modulus (G' , \blacktriangle) and loss modulus (G'' , \times) of 60% L81 (\bullet), 70% L92 (\bullet), 70% L92-NH₂ (\bullet).

G' and G'' occur at 5.6%, 5.1%, and 6.2% for 70% L92-NH₂, 70% L92 and 60% L81, respectively.

70% L92-NH₂ displays strain-thinning behavior, also called LAOS type I, because both G' and G'' decrease with increasing strain. In the same way as the shear-thinning behavior discussed above, the decrease of G' and G'' is caused by the disentanglement of the polymer chains and the alignment of the chains in the flow direction [32]. On the other hand, 70% L92 and 60% L81 follow LAOS type III behavior because G' decreases, whereas G'' shows a weak strain overshoot [31, 32]. The small increase in G'' is caused by the breakage of the connections between aggregates, but as the strain keeps increasing, the lamellar phases slide against each other, leading to a decrease in G'' [31].

Frequency sweep. Fig. 9 shows the results of the frequency sweep conducted at 0.1% strain of the three liquid-crystalline samples. The crossover points of 70% L92-NH₂, 70% L92, and 60% L81 are found at 36.6, 15.6, and 10.6 Hz, respectively. In all cases G' and G'' increase up to the crossover point, although the increase of G'' is steeper. For most of the studied frequency range, the samples exhibit elastic behavior. 60% L81 has the shortest relaxation time, followed by 70% L92, and 70% L92-NH₂, meaning that 60% L81 has the strongest viscous component. These results are in agreement with the trends observed in the viscosity measurements of the samples. The decrease in G' of 70% L92 and 60% L81 after the crossover is caused by inertia effects [59].

NMR experiments

Fig. 10 shows the distribution of water diffusion coefficients in three different LCs obtained from PFG NMR diffusion experiments. Even though the spectra seem to provide two distinct distributions, the attenuation of the slow diffusing phase is not strong

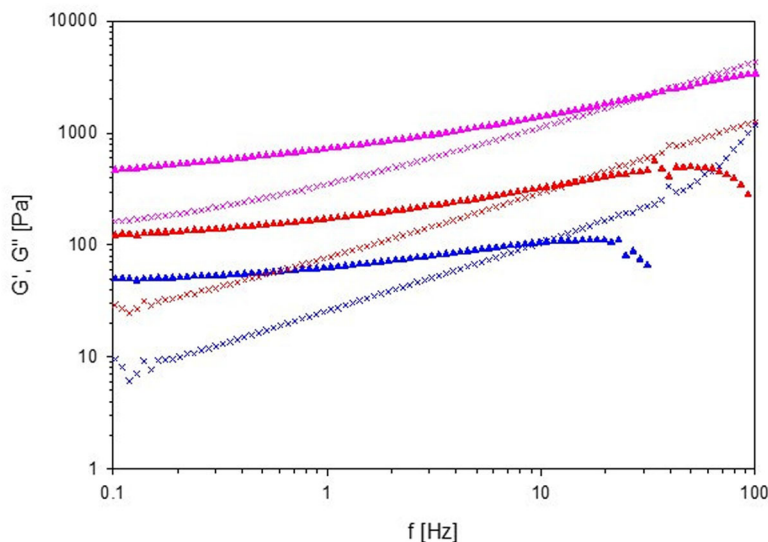


Figure 9. Storage modulus (G' , \blacktriangle) and loss modulus (G'' , \times) of 60% L81 (\bullet), 70% L92 (\bullet), 70% L92-NH₂ (\bullet).

enough to conclude that the shape of the distributions is as shown in Fig. 10. However, the attenuation is strong enough to conclude that the average mobility of the slow diffusing phase is of the order of 10^{-12} m²/s. Therefore, the data obtained from the NMR experiments are only used to qualitatively assess the behavior of water in the LCs.

The NMR spectra of the studied LCs show two distinct regions: below 10^{-10} m²/s the peaks represent water molecules that are tightly bound to the polymer, and above the 10^{-10} m²/s threshold, water with higher mobility. In general, the water with low mobility could be trapped inside polymer aggregates or have hindered mobility in some other way. On the other hand, high mobility water could be water located in between polymer aggregates. In these cavities the water moves more freely and consequently exhibits a higher mobility. The three systems present phase separation at 55 °C due to the decrease in solubility of both the PEO and PPO blocks [45]. PPO has a hydrophobic nature, whereas PEO segments adopt a less polar configuration at higher temperatures, thereby reducing their water solubility. This results in a two-phase system where there is a polymer-rich phase with disorganized microstructure, and an aqueous phase. In the cases of both 60% L81 and 70% L92 the overall mobility of water increases when the temperature is increased from 25 to 55 °C. This behavior is consistent with the phase separation that occurs upon heating the polymer solution, which would lead to an increase in water mobility in the system, and with the general increase of diffusion with higher temperature [24, 60, 61]. In the case of 70% L92-NH₂, when the temperature is increased from 25 to 55 °C the mobility of water decreases. However, a small peak also appears at high diffusion coefficients, indicating that there is a small portion of water molecules with increased mobility. The shift of the two main peaks at 55 °C to lower diffusion coefficients could be caused by trapping water inside the polymer aggregates when these aggregates collapse. The peak at 10^{-9} m²/s would correspond to highly mobile water from the phase separation. This would indicate that the temperature

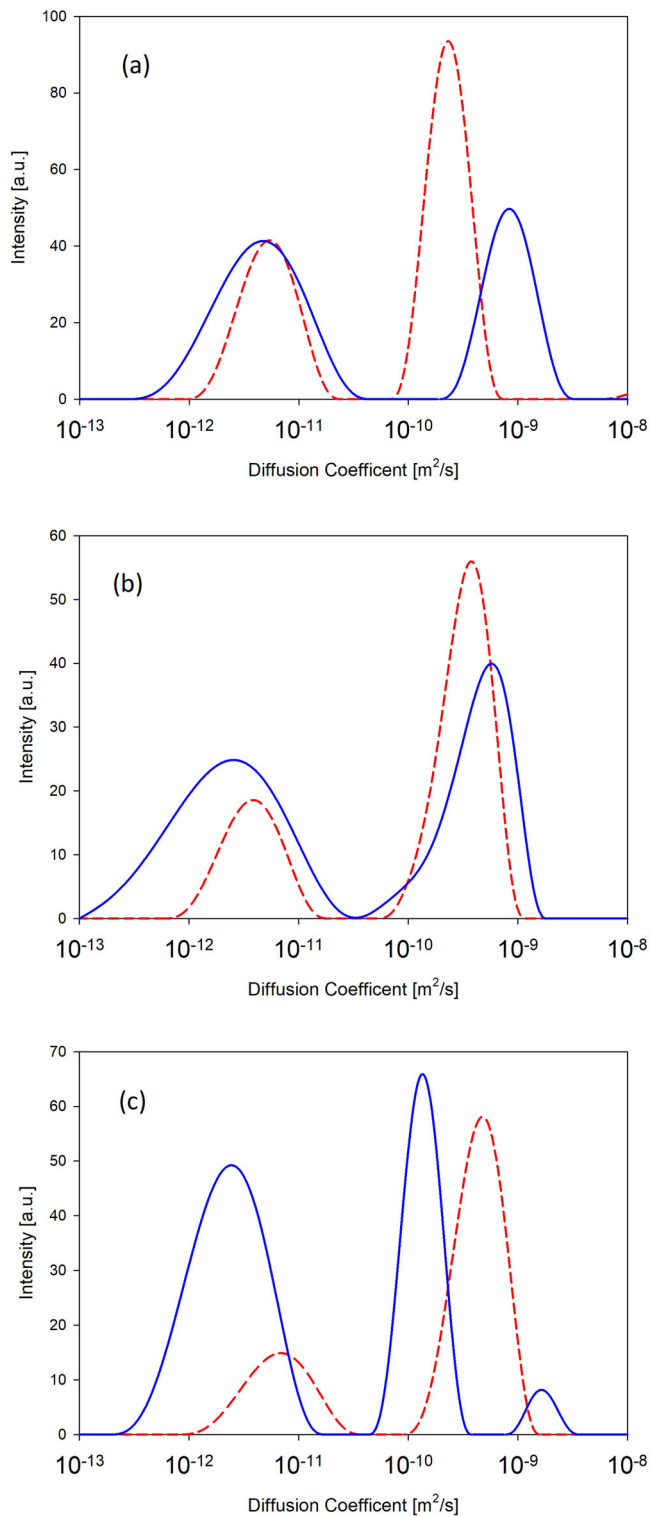


Figure 10. Distribution of water diffusion coefficients in (a) 60% L81, (b) 70% L92, and (c) 70% L92-NH₂ at 25 (dashed line) and 55 °C (solid line).

induced collapse of the polymer aggregates leaving water-filled “voids” between the aggregates, or in other words pushing water out of the polymer aggregates without inducing (visible) phase separation. Although water diffusion does not provide direct information about CO₂ absorption in the investigated LCs, it indicates the mobility of molecules within the LCs. This information is useful to assess whether carbon dioxide can diffuse through the LCs. In principle, since there is a large amount of loosely bound water, this would allow CO₂ to penetrate through the LCs, up to a certain point, because diffusion through some domains would be “blocked” by tightly bound water. On the other hand, water molecules form hydrogen bonds with the polymer molecules, leading to a decrease in the ether groups available to form quadrupole interactions with CO₂, and thus preventing CO₂ from also interacting with the polar groups in the polymers [62]. Therefore, tightly bound water not only hinders the diffusion of CO₂ within the LCs, but also prevents CO₂ from interacting with the polymer, which reduces the overall CO₂ absorption.

Conclusions

This article reports the CO₂-absorption of three different LCs (60% L81, 70% L92, and 70% L92-NH₂) as well as the viscosity of these systems, and the water diffusion within the samples at 25 and 55 °C. L92-NH₂ was obtained via a two-step modification of L92 with a yield of 59–67%, and an overall end-group conversion of 34%. Samples of 70% L92-NH₂ presented a transition from lamellar to (reverse) hexagonal phase when the temperature increased from 20 to 25 °C. The loading of the LCs was recorded up to 6 bar and was compared with the loading of the pure polymers at the same conditions (L81 and L92). In addition, the viscosity of the samples was measured. A correlation between the loading and the viscosity of the samples was observed within samples of the same polymer, where the most viscous samples displayed the lowest CO₂-loading (α : 70% L92-NH₂ < 70% L92 < L92, and 60% L81 < L81). In addition, the effects of the hydrophilicity of the samples were observed: 70% L92 and L92, reached higher loadings than 60% L81 and L81, respectively, even though L92 samples are more viscous. Therefore, one can conclude that lower viscosity and higher hydrophilicity (higher EO content) contribute to increase the loading of the samples. In addition, the ionic strength of the samples might play a role in the CO₂ absorption. The viscosity of the LCs was also measured after CO₂ absorption, showing no changes in the viscosity. Finally, the diffusion of water in the LCs was studied by NMR. Two distinct signals were observed: one corresponding to tightly bound/trapped water (low diffusion coefficient), and one corresponding to water confined in larger cavities (yields higher diffusivity). Upon increasing the temperature, the polymers aggregate and phase separate, leading to increased mobility of water. However, in 70% L92-NH₂ the two main peaks appear at lower diffusion coefficient values while a small peak of high mobility water appears, suggesting that phase separation is not complete. Overall, the results obtained in this work suggest that LCs are not a competitive alternative to traditional solvents used in CCS. However, the results that we report (regarding the absorption of the LCs), are in agreement with the results available in the literature for other LC systems.

Disclosure statement

No potential conflict of interest was reported by the author(s).

Funding

This work was supported by the Research Council of Norway under the CLIMIT-program (grant 239778) with an included matching funding contribution by Gassnova SF.

ORCID

Sandra Rodríguez-Fabià  <https://orcid.org/0000-0002-4273-231X>

Hanna K. Knuutila  <http://orcid.org/0000-0003-2057-1743>

Kristofer Gunnar Paso  <http://orcid.org/0000-0002-0502-9780>

References

- [1] J. Gross, and P. J. Jansens, *European Patent Office* NL (4 Dec. 2008).
- [2] M. de Groen, T. J. H. Vlugt, and T. W. de Loos, *J. Phys. Chem. B* 116 (30), 9101 (2012). doi:10.1021/jp303426k
- [3] M. De Groen *et al.*, *J. Chem. Thermodyn.* 59, 20 (2013). doi:10.1016/j.jct.2012.11.026
- [4] M. de Groen *et al.*, *J. Chem. Eng. Data* 59 (5), 1667 (2014). doi:10.1021/je500124r
- [5] M. de Groen, T. J. H. Vlugt, and T. W. de Loos, *AIChE J.* 61 (9), 2977 (2015). doi:10.1002/aic.14857
- [6] *IPCC Special Report on Carbon Dioxide Capture and Storage*. Prepared by Working Group III of the Intergovernmental Panel on Climate Change (Cambridge University Press, Cambridge, United Kingdom and New York, USA 2005).
- [7] A. A. Olajire, *Energy* 35 (6), 2610 (2010). doi:10.1016/j.energy.2010.02.030
- [8] J. Gibbins, and H. Chalmers, *Energy Policy* 36 (12), 4317 (2008). doi:10.1016/j.enpol.2008.09.058
- [9] D. M. D'Alessandro, B. Smit, and J. R. Long, *Angew Chem. Int. Edit* 49, 6058 (2010). doi:10.1002/anie.201000431
- [10] J. G. J. Olivier, K. M. Schure, and J. A. H. W. Peters, *Trends in Global CO₂ and Total Greenhouse Gas Emissions 2017 Report* (The Hague, Netherlands: Pbl 2017).
- [11] IPCC, Summary for Policymakers, in *Global Warming of 1.5°C. An IPCC Special Report on the Impacts of Global Warming of 1.5°C above Pre-Industrial Levels and Related Global Greenhouse Gas Emission Pathways, in the Context of Strengthening the Global Response to the Threat of Climate Change, Sustainable Development, and Efforts to Eradicate Poverty* (World Meteorological Organization, Geneva, Switzerland 2018).
- [12] D.-S. Chen *et al.*, *Mol. Cryst. Liq. Crys. A* 237 (1), 85 (1993). doi:10.1080/10587259308030126
- [13] G.-H. Hsiue, D.-S. Chen, and C.-J. Hsieh, *Mol. Cryst. Liq. Crys. A* 241 (1), 187 (1994). doi:10.1080/10587259408029755
- [14] G.-H. Chen, and J. Springer, *Mol. Cryst. Liq. Crys. A* 339 (1), 31 (2000). doi:10.1080/10587250008031030
- [15] D.-S. Chen, and G.-H. Hsiue, *Polymer* 35 (13), 2808 (1994). doi:10.1016/0032-3861(94)90310-7
- [16] M. De Groen *et al.*, *J. Chem. Eng. Data* 60 (7), 2167 (2015). doi:10.1021/acs.jced.5b00295
- [17] L. Coppola *et al.*, *Colloid Polym. Sci.* 278 (5), 434 (2000). doi:10.1007/s003960050536
- [18] S.-Z. Zu, and B.-H. Han, *J. Phys. Chem. C* 113 (31), 13651 (2009). doi:10.1021/jp9035887

- [19] S. Lee *et al.*, *Macromolecules* 37 (22), 8349 (2004). doi:10.1021/ma049076w
- [20] M. Wulff-Pérez *et al.*, *Food Hydrocoll.* 23 (4), 1096 (2009). doi:10.1016/j.foodhyd.2008.09.017
- [21] E. V. Batrakova, and A. V. Kabanov, *J. Control. Release.* 130 (2), 98 (2008). doi:10.1016/j.jconrel.2008.04.013
- [22] BASF, *Pluronic PE types -Technical Information* (BASF, Ludwigshafen, Germany 1996).
- [23] J. Noolandi, A.-C. Shi, and P. Linse, *Macromolecules* 29 (18), 5907 (1996). doi:10.1021/ma960272f
- [24] M. Svensson, P. Alexandridis, and P. Linse, *Macromolecules* 32 (3), 637 (1999). doi:10.1021/ma9812940
- [25] S. Yang *et al.*, *Colloids Surf. A* 322 (1–3), 87 (2008). doi:10.1016/j.colsurfa.2008.02.029
- [26] G. Wanka, H. Hoffmann, and W. Ulbricht, *Macromolecules* 27 (15), 4145 (1994). doi:10.1021/ma00093a016
- [27] K. Zhang, and A. Khan, *Macromolecules* 28 (11), 3807 (1995). doi:10.1021/ma00115a009
- [28] O. Robles-Vásquez *et al.*, *J. Colloid Interface Sci.* 160 (1), 65 (1993). doi:10.1006/jcis.1993.1368
- [29] R. Mezzenga *et al.*, *Langmuir* 21 (8), 3322 (2005). doi:10.1021/la046964b
- [30] R. K. Prud'homme, G. Wu, and D. K. Schneider, *Langmuir* 12 (20), 4651 (1996). doi:10.1021/la951506b
- [31] K. Hyun *et al.*, *Rheol. Acta* 45 (3), 239 (2006). doi:10.1007/s00397-005-0014-x
- [32] K. Hyun *et al.*, *J. Non-Newtonian Fluid Mech.* 107 (1–3), 51 (2002). doi:10.1016/S0377-0257(02)00141-6
- [33] A. V. Rayer, A. Henni, and P. Tontiwachwuthikul, *Can. J. Chem. Eng.* 90 (3), 576 (2012). doi:10.1002/cjce.20615
- [34] J. Li *et al.*, *J. Chem. Eng. Data* 57 (2), 610 (2012). doi:10.1021/je201197m
- [35] E. Weidner *et al.*, *J. Supercrit. Fluids* 10 (3), 139 (1997). doi:10.1016/S0896-8446(97)00016-8
- [36] V. Wiesmet *et al.*, *J. Supercrit. Fluids* 17 (1), 1 (2000). doi:10.1016/S0896-8446(99)00043-1
- [37] S. Choi, J. H. Drese, and C. W. Jones, *ChemSusChem.* 2, 796 (2009). doi:10.1002/cssc.200900036
- [38] J. C. Hicks *et al.*, *J. Am. Chem. Soc.* 130 (10), 2902 (2008). doi:10.1021/ja077795v
- [39] H.-S. Choi, and M. P. Suh, *Angewandte Chemie International Edition.* 48, 6865 (2009). doi:10.1002/anie.200902836
- [40] S. Ben Hamouda *et al.*, *CR. Chim.* 13 (3), 372 (2010). doi:10.1016/j.crci.2009.10.009
- [41] J. M. Harris *et al.*, *J. Polym. Sci. Polym. Chem. Ed.* 22 (2), 341 (1984). doi:10.1002/pol.1984.170220207
- [42] G. Gyulai *et al.*, *Express Polym. Lett.* 10 (3), 216 (2016). doi:10.3144/expresspolymlett.2016.20
- [43] A. V. Kabanov, E. V. Batrakova, and V. Y. Alakhov, *J. Control. Release.* 82 (2–3), 189 (2002). doi:10.1016/s0168-3659(02)00009-3
- [44] D. B. G. Williams, and M. Lawton, *J. Org. Chem.* 75 (24), 8351 (2010). doi:10.1021/jo101589h
- [45] P. Alexandridis, D. Zhou, and A. Khan, *Langmuir* 12 (11), 2690 (1996). doi:10.1021/la951025s
- [46] S. Evjen *et al.*, *Int. J. Greenhouse Gas Control.* 76, 167 (2018). doi:10.1016/j.ijggc.2018.06.017
- [47] G. H. Sørland, B. Hafskjold, and O. Herstad, *J. Magn. Reson.* 124 (1), 172 (1997). doi:10.1006/jmre.1996.1029
- [48] G. H. Sørland, *Dynamic Pulsed-Field-Gradient NMR* (Springer- Verlag, Berlin Heidelberg Germany 2014).
- [49] G. H. Sørland, *AIP Conf. Proceed.* 1330, 27 (2011). doi:10.1063/1.3562225
- [50] S. Rodríguez-Fabià *et al.*, *Polymers* 11 (2), 309 (2019). doi:10.3390/polym11020309
- [51] S. De Bernardo *et al.*, *Arch. Biochem. Biophys.* 163 (1), 390 (1974). doi:10.1016/0003-9861(74)90490-1

- [52] S. Rodríguez-Fabià *et al.*, *Polymers* 10 (8), 883 (2018). doi:[10.3390/polym10080883](https://doi.org/10.3390/polym10080883)
- [53] O. Aschenbrenner, and P. Styring, *Energy Environ. Sci.* 3 (8), 1106 (2010). doi:[10.1039/c002915g](https://doi.org/10.1039/c002915g)
- [54] P. D. Vaidya, and E. Y. Kenig, *Chem. Eng. Technol.* 30 (11), 1467 (2007). doi:[10.1002/ceat.200700268](https://doi.org/10.1002/ceat.200700268)
- [55] G. Montalvo, M. Valiente, and E. Rodenas, *Langmuir* 12 (21), 5202 (1996). doi:[10.1021/la9515682](https://doi.org/10.1021/la9515682)
- [56] G. Harrison *et al.*, *Korea-Aust. Rheol. J.* 11, 197 (1999).
- [57] M. Sveistrup *et al.*, *J. Dispersion Sci. Technol.* 37 (8), 1160 (2016). doi:[10.1080/01932691.2015.1088450](https://doi.org/10.1080/01932691.2015.1088450)
- [58] V. M. Ugaz, D. K. Cinader, and W. R. Burghardt, *Macromolecules* 30 (5), 1527 (1997). doi:[10.1021/ma961759r](https://doi.org/10.1021/ma961759r)
- [59] J. Läger, and H. Stettin, *Journal of Rheology*. 60, 393 (2016). doi:[10.1122/1.4944512](https://doi.org/10.1122/1.4944512)
- [60] I. R. Schmolka, *J. Am. Oil Chem. Soc.* 54 (3), 110 (1977). doi:[10.1007/BF02894385](https://doi.org/10.1007/BF02894385)
- [61] M. Kell, *J. Phys: Condens. Matter* 8, A103 (1996). doi:[10.1088/0953-8984/8/25A/008](https://doi.org/10.1088/0953-8984/8/25A/008)
- [62] R. Nagumo *et al.*, *Ind. Eng. Chem. Res.* 55 (29), 8200 (2016). doi:[10.1021/acs.iecr.6b01074](https://doi.org/10.1021/acs.iecr.6b01074)
- [63] Z. Duan, and R. Sun, *Chem. Geol.* 193 (3–4), 257 (2003). doi:[10.1016/S0009-2541\(02\)00263-2](https://doi.org/10.1016/S0009-2541(02)00263-2)